Model Selection for Range Segmentation of Curved Objects

Alireza Bab-Hadiashar and Niloofar Gheissari

School of Engineering & Science, Swinburne University of Technology,
Melbourne, Australia
{Abab-hadiashar,ngheissari}@swin.edu.au

Abstract. In the present paper, we address the problem of recovering the true underlying model of a surface while performing the segmentation. A novel criterion for surface (model) selection is introduced and its performance for selecting the underlying model of various surfaces has been tested and compared with many other existing techniques. Using this criterion, we then present a range data segmentation algorithm capable of segmenting complex objects with planar and curved surfaces. The algorithm simultaneously identifies the type (order and geometric shape) of surface and separates all the points that are part of that surface from the rest in a range image. The paper includes the segmentation results of a large collection of range images obtained from objects with planar and curved surfaces.

1 Introduction

Model selection has received substantial attention in the last three decades due to its various applications in statistics, engineering and science. During this time, many model selection criteria (Table 1) have been proposed, almost all of which have their roots in statistical analysis of the measured data. In this paper we propose a new approach to the model selection problem based on physical constraints rather than statistical characteristics. Our approach is motivated by our observations that none of the existing model selection criteria is capable of reliably recovering the underlying model of range data of curved objects (see Figure 1).

Before we explain our model selection criterion, the problem of range segmentation for none-planar objects is briefly reviewed in the next section. Later, we propose a novel model selection tool called Surface Selection Criterion (SSC). This proposed criterion is based on the minimisation of the bending and twisting energy of a thin surface. To demonstrate the effectiveness of our proposed SSC, we devised a robust model based range segmentation algorithm for curved objects (not limited to planar surfaces). The proposed Surface Selection Criterion allows us the to choose the appropriate surface model from a library of models. An important aspect of having a correct model is obtaining the surface parameters while segmenting the surface. Recovering the underlying model is a crucial aspect of segmentation when the objects are not limited to having planar surfaces only (so more than one possible candidate exists).

T. Pajdla and J. Matas (Eds.): ECCV 2004, LNCS 3021, pp. 83–94, 2004.

Table 1. Different model selection criteria studied in this paper, N is the number of points and P is the number of parameters. J is the fisher matrix of the estimated parameters. L is equal to N. d is the dimension of manifold (here 2) and m is the dimension of the data. (here 3). f is the degrees of freedom of the assumed t distribution for MCAIC (here 1.5)

Name	Criterion
MDL[24]	$\sum_{i=1}^{n} r_i^2 + (P/2)\log(N)\delta^2$
GBIC[6]	$\sum_{i=1}^{n} r_i^2 + (Nd\ \log(4) + P\log(4N))\delta^2$
CP Kanatani [15]	$\sum_{i=1}^{n} r_i^2 + (2(dN + P) - mN)\delta^2$
CP Mallow [19]	$\sum_{i=1}^{n} r_i^2 + (-N + 2P)\delta^2$
GAIC[16]	$\sum_{i=1}^{n} r_i^2 + 2(dN + P)\delta^2$
SSD[25]	$\sum_{i=1}^{n} r_i^2 + (P\log(N+2)/24 + 2\log(p+1))\delta^2$
CAIC[5]	$\sum_{i=1}^{n} r_i^2 + P(\log N + 1)\delta^2$
CAICF[5]	$\sum_{i=1}^{n} r_i^2 + P(\log N + 2)\delta^2 + \log\lvert J\rvert$
GMDL[16]	$\sum_{i=1}^{n} r_i^2 - (Nd + P)\varepsilon^2 \log(\varepsilon/L)^2$
MCAIC [4]	$(1+f)\sum_{i=1}^{n} w_i \log\left[1 + \frac{r_i^2}{f\delta^2}\right] P(\log N + 1)\delta^2$

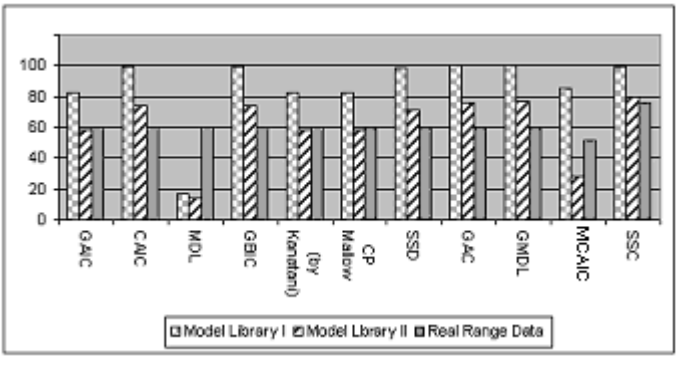

Fig. 1. Comparison of various model selection criteria for synthetic and real range data

2 Range Segmentation

A range image contains 3D information about a scene including the depth of each pixel. Segmenting a range image is the task of dividing the image into regions so that all the points of the same surface belong to the same region, there is no overlap between different regions, and the union of these regions generates the entire image.

There have been two main approaches to address the range segmentation problem. The first one is the region-based approach, in which, one groups data points so that all of them can be regarded as members of a parametric plane ([18] or [3]). The other approach is based on the edge detection and labelling edges using the jump edges (discontinuities). For example, [8] or [14].

Although the range image segmentation problem has been studied for number of years, the task of segmenting range images of curved surfaces is yet to be satisfactorily resolved. The comparative survey of Powell et al. [23] indeed reveals the challenges that need to be addressed. An early work in the area of segmentation of curved surfaces was published in 1994 by Boyer et al. [4]. They used a modified version of Bozdogan's CAIC [5] as a model selection criterion. Later, Besel and Jain [3] proposed a range image segmentation algorithm to segment range images of curved objects. The performance of their proposed algorithm for segmenting curved surfaces has been reported (by Powel et al. [23]) as unsatisfactory in many cases. Bab-Hadiashar and Suter [2] have also proposed a segmentation algorithm, which was capable of segmenting a range image of curved objects. Although they managed to segment range images into regions expressed by a specific quadratic surface, their method was limited, as it could not distinguish between different types of quadratic surfaces. Although there have been other attempts to segment range data using higher order surfaces [11,20,22,28], there have been few range segmentation algorithms capable of successfully segmenting curved objects and recovering the order of those segments. A complete literature review on range segmentation is beyond the scope of this paper. A comprehensive survey and comparison of different range segmentation algorithms was reported by Hoover et al. [13]; While a survey on model-based object recognition for range images has been reported by Arman and Aggarwal [1].

In this paper, we propose a range segmentation algorithm that is capable of identifying the order of the underlying surface while calculating the parameters of the surface. To accomplish this, we propose a new model selection criterion called Surface Selection Criterion to recover the correct surface model while segmenting the range data. An important aspect of our segmentation algorithm is that it can solve occlusion properly (it will be described in the step 6 of the segmentation algorithm). To evaluate and compare the performance of our algorithm with other existing range segmentation algorithms, we have first tested the proposed algorithm on the ABW image database [12]. The results of these experiments are shown in experimental results. Since the ABW database does not contain images of curved objects, we then created a range image database of a number of objects possessing both planar and curved surfaces. The results of those experiments (shown in Figure 1) confirm that our algorithm is not only capable of segmenting planar surfaces but can also segment higher order surfaces correctly.

3 Model Selection

In this section we propose a Surface Selection Criterion to identify the appropriate model from a family of models representing possible surfaces of a curved object. Our proposed criterion is based on minimising the sum of bending and twisting energies of all possible surfaces. Although, the bending energy of a surface has been used in the literature for motion tracking and finding parameters of deformable objects ([29] [30] [7]) and also in shape context matching and active contours([17]), it hasn't been used for model selection purposes.

3.1 Our Proposed Surface Selection Criterion

Our proposed criterion is based on minimising the sum of bending and twisting energy of all possible surfaces in a model library. To formulate our model selection criterion, we view the range data of different points of an object as hypothetical springs constraining the surface. If the surface has little stiffness, then the surface passes close to measurements (fits itself to the noise) and the sum of squared residuals between the range measurements and their associated points on the surface will be small (the sum of squared residuals in this analogy, relates to the energy of the deformed springs). However, to attain such proximity, the surface has to bend and twist in order to be close to the measured data. This in turn increases the amount of strain energy accumulated by the surface. For model selection, we propose to view the sum of bending and twisting energies of the surface as a measure of surface roughness and the sum of squared residuals as a measure of fidelity to the true data. A good model selection criterion should therefore represent an acceptable compromise between these two factors. As one may expect, increasing the number of parameters of a surface leads to a larger bending and twisting energies as the surface has more degrees of freedom and consequently the surface can be fitted to the data by bending and twisting itself so that a closer fit to measured data results (this can be inferred from the bending energy formula (Equation 1). However, the higher the number of parameters for a surface model assumed, the less the sum of squared residuals is going to be. For instance, in the extreme case, if the number of parameters is equal to the number of data points (which are used in the fitting process), then the sum of squared residuals will be zero whereas its sum of energies will be maximised.

We have a conjecture as to why this approach should be advantageous. Common statistical methods that rely essentially on probability distribution of residuals ignore spatial distribution of the deviations of data points from the surface. Whereas the above method intrinsically (through a physical model) couples the local spatial distribution of residuals to the strain energy in that locality. We argue that this is an important point as the range measurements are affected by localised factors (such as surrounding texture, surface specularities, etc) as well as by the overall accuracy and repeatability of the rangefinders.

As shown in [27], if a plate is bent by a uniformly distributed bending moment so that the xy and yz planes are the principal planes of the deflected surface, then the strain energy (for bending and twisting) of the plate can be expressed as:

$$E_{Bending+Twist} = \iint_s \frac{1}{2} D\left\{ \left(\frac{\partial^2 w}{\partial x^2} + \frac{\partial^2 w}{\partial y^2}\right)^2 - 2(1-\nu)\left[\frac{\partial^2 w}{\partial x^2}\frac{\partial^2 w}{\partial y^2} - \left(\frac{\partial^2 w}{\partial x \partial y}\right)^2\right]\right\} dxdy$$

Equation 1

where D is the flexural rigidity of the surface and v is Poisson's ratio (v should be very small because in real world-objects the twisting energy in comparison with the bending energy is small). In our experiments we assume $\nu = 0.01$. We found in our experiments that the performance of SSC is not overly sensitive to the small variation of this value. In order to scale the strain energy, we divide its value by the strain energy of the model with the highest number of parameters ($E_{\max}$). Therefore, D will be eliminated from our computation.

To capture the trade-off between the sum of squared residuals $\sum_{i=1}^{N} r_i^2$ and the strain energy $E_{\text{Bending+Twist}}$, we define a function *SSC* such that:

$$SSC = \sum_{i=1}^{N} r_i^2 / N\delta^2 + P\frac{E_{Bending+Twist}}{E_{\max}}$$

where δ is the scale of noise for the highest surface (the surface with the highest number of parameters). The reason that we use the scale of noise for the highest surface (as explained by Kanatani [15]) is that the scale of noise for the correct model and the scale of noise of the higher order models (higher than the correct model) must be close for the fitting to be meaningful. Therefore, it is the best estimation of the true scale of noise which is available at this stage. The energy term has been multiplied by the number of parameters P in order to discourage choosing a higher order (than necessary) model. Such a simple measure produces good discrimination and improves the accuracy of the model selection criterion. Having devised a reasonable compromise between fidelity to data and the complexity of the model, our model selection task is then reduced to choosing the surface that has the minimum value of SSC. To evaluate our proposed Surface Selection Criterion and compare it with other well known model selection criteria (Table 1), we first created five synthetic data sets according to the surface models in Surface Library 1 (one for each model) and randomly changed the parameters of each data set 1000 times. We also added 10% normally distributed noise. The success rates of all methods in correctly recovering the underlying model are shown in Figure 1. To consider more realistic surfaces, we then considered a more comprehensive set of surface models (shown in Surface Library 2) and repeated the above experiments. The percentages of successes in this case are also shown in Figure 1.

Finally, to examine the success rate of our Surface Selection Criterion and compare it with other selection techniques on real range images, we randomly hand picked points of 100 planar surfaces of the objects in ABW range image database [12] and also 48 curved (quadratic) surfaces of our range image database. In this case, the model library used is the Surface Library 3. The results are also shown in Figure 1.

As can be seen from Figure 1, the proposed criterion (SSC) is considerably better in choosing the right model when it is applied to a variety of real range data. We should note here that the performance of MCAIC [4] is expected to be slightly better than what we have reported here if the segmentation frame work reported in [4] is used (here, we only examined the selection capability of the criteria).

Surface Library 1

Model 1	$z=ax^2+by^2+cxy+dx+ey+f$
Model 2	$z=ax^2+bxy+cx+dy+e$
Model 3	$z=ax^2+by^2+cx+dy+e$
Model 4	$z= axy+bx+cy+d$
Model 5	$z=ax+by+c$

Surface Library 2. (It should be noted that bending energy is shift and rotation invariant. Therefore there is no need to add more models to this library that have other possible combinations of x, y and z)

Model 1	$ax^2+by^2+cz^2+dxy+eyz+fxy+gx+hy+iz=1$
Model 2	$ax^2+by^2+cxy+dyz+exy+fx+gy+hz=1$
Model 3	$ax^2+by^2+cz^2+dx+ey+fz=1$
Model 4	$axy+byz+cxy+dx+ey+fz=1$
Model 5	$ax^2+by^2+cz^2+dxy+eyz+fxy=1$
Model 6	$ax^2+by^2+cx+dy+ez=1$
Model 7	$ax+by+cz=1$

Surface Library 3

Model 1	$ax^2+by^2+cz^2+dxy+eyz+fxy+gx+hy+iz=1$
Model 2	$ax^2+by^2+cz^2+dx+ey+fz=1$
Model 3	$ax+by+cz=1$

However, to improve the efficiency of our proposed Surface Selection Criterion, we can carry out some post processing, provided that we have a set of nested models in the model library (like Surface Library 2).

That is if the sum of squares of non-common terms between the higher surface and the next lower surface is less than a threshold, we select the lower surface. This simple step also improves the already high success rate of our proposed SSC.

4 Segmentation Algorithm

Having found a reliable method for recovering the underlying model of a higher order surface, we then proceed to use this method to perform the range segmentation of curved objects. Since our segmentation algorithm requires an estimate of the scale of noise, we have implemented the method presented in [2].

4.1 Model Based Range Segmentation Algorithm

In this section, we briefly but precisely, explain the steps of the proposed range segmentation algorithm. The statistical justification of each step is beyond the scope

of this paper but it is suffice to mention that the algorithm has been closely modelled on the ones presented in [21,26] for calculating the least median of squares. The proposed algorithm combines the above noise estimation technique and our model selection criterion SSC and delivers an effective mean for segmenting not only planar objects (as can be seen from our experiments with ABW range data) but also curved objects containing higher order models. This algorithm has been extensively tested on several range data images with considerable success (presented in experimental results). The required steps are as follows:

1. Eliminate pixels whose associated depths are not valid due to the limitation of the range finder used for measuring the depth (mainly due specularities, poor texture, etc). These points are usually marked by the range scanner with an out-of-range number. If there are no such points we can skip this stage.

2. Find a localised data group inside the data space in which all the pixels appear on a flat plane. Even if there is no planar surface in the image, we can always approximate a very small local area (here 15×15) as a planar surface. To implement this stage and find such a data group, we choose a number of random points, which all belong to the same square of size R (this square is only for the sake of local sampling). Using these points, create an over-determined linear equation system. If the number of inliers is more than half of the size of the square, then, mark this square as an acceptable data group. The size of the square (R) is not important, however it needs to be large enough to contain adequate sample points. We set the square size as 15×15 in our experiments. We have chosen this size because a square of size 15×15 can contain enough samples. In our experiments, 30 samples were used to perform the above step.

3. Fit the highest model in the library to all the accepted data groups and find the residual for each point. Then, repeat the above two steps and accept the data group that has the least K^{th} order residual (the choice of K depends on the application [2] and is set to 10% for our experiments). This algorithm is not sensitive to the value of K. However, if we assume K to be very large, small structures will be ignored.

4. Apply a model selection method (here SSC) to the extended region (by fitting and comparing all models in the model library to the extended region) and find the appropriate model.

5. Fit the chosen model to the whole data (not segmented parts); compute the residuals and estimate the scale of noise using the technique explained in the previous section. In the next step this scale will help us to reject the outliers. It is important to note that performing this step has the advantage that it can also remedy the occlusion problem if there is any. This means that if a surface of an object is divided - occluded - by another object, we can then rightly join the separated parts as one segment.

6. Establish a group of inliers based on the obtained scale and reject the outliers. We reject those points whose squared residual is greater than the threshold T^2 multiple of the scale of noise (see the inequality $r^2_{n+1} > T^2\ \delta^2$ in the previous section). Then, recalculate the residuals and compute the final scale using: $\delta^2 = \sum_{i=1}^{n} r_i^{\,2} / (N - P)$.

7. Apply a hole-filling (here, we use a median filter of 10 by 10 pixels) algorithm to all inliers and remove holes resulting from invalid and noisy points (points where the

range finder has not been able to correctly measure the depth mainly due to their surface texture). This step is only for the sake of the appearance of the results and has no effect on the segmented surface's parameters because the fitting has already been performed. However, some of the missed invalid, and noisy points can be grouped in this step. This step is not essential and can be skipped if desired.

8. Eliminate the segmented part from the data.

9. Repeat the steps 1 to 8 until the number of remaining data becomes less than the size of the smallest possible region in the considered application.

5 Experimental Results on Segmentation

To evaluate the performance of the proposed algorithm, we have conducted a comprehensive set of experiments using real range images of various objects. The first set of experiments is solely for comparison purposes and is performed on the existing ABW database that only includes objects with planar surfaces. It is shown that the proposed technique can accurately segment the above database and its performance is similar to the best techniques presented in the literature [13]. We have then applied our technique to a set of real range images with objects having a combination of planar and curved surfaces. By these experiments we have shown that the present technique is not only capable of segmenting these objects correctly, but also truly identifies the underlying model of each surface.

5.1 ABW Image Database

In the first set of our experiments, we applied our algorithm on the ABW[12] range image database and compared our results with the ones reported by Hoover et al. [13]. As is shown here, the proposed technique is able to segment all of the images, correctly. Less than 1% of over-segmentation has occurred which is in turn resolved by using a simple merging (post-processing) step. To show the performance of our algorithm in estimating angles and comparing it with the results obtained by Hoover et al. [13], we randomly chose 100 surfaces and calculated the absolute difference between the real angle (calculated using the IDEAS CAD package) and the computed angle using the parameters of the segmented surface. The average and the standard deviation of the error for our technique and others reported in the literature are shown in Table 2. A few of the results of segmenting the ABW range image database are shown in Fig. 2.

Table 2. Comparison of accuracy of estimated angles

Technique	Angle diff. (std dev.)
USF[10]	1.6(0.8)
WSU[11]	1.6(0.7)
UB[14]	1.3(0.8)
UE[9,28]	1.6(0.9)
Proposed algorithm	1.4(0.9)

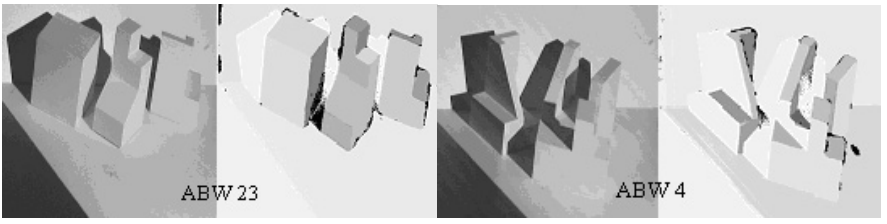

Fig. 2. Left: intensity image. Right: segmentation result

5.2 Curved Objects Database

To evaluate the performance of our algorithm in segmenting range images of curved objects, we created a range image database of a number of objects possessing both planar and curved surfaces. The actual data and their segmented results are shown in the following figures (Figure 3 to 9). We use a comprehensive model library (Surface Library 4), which consists of the most concise possible model for each object in the scene. For example, because we have cylinders (or part of) perpendicular to the xy plane in our objects, then the model $ax^2 + by^2 + cx + dy = 1$ is included in the model library (Surface Library 4).

Our segmentation algorithm was able to correctly identify the underlying model for each surface using Surface Library 4 as our model library, and SSC as a model selection criterion. The following figures shows the results of our experiments. In all of these figures, the labels show the underlying detected model. The algorithm has been successfully labeling all surfaces. For example surface 11,14,15,16, and 4 in Fig. 3 and Fig. 4, which are cylinders *perpendicular* to the xy plane, are identified to have the underlying Model 5. The underlying model for surface 25 in Fig. 6 was chosen to be Model 3, which is a cylinder *parallel* to the xy plane. Therefore our method not only can detect the cylindrical shape of the surface but it is also able to distinguish the direction of cylinders (detecting the degeneracy). For all flat surfaces SSC truly selects model 8, which represents a flat plane. An advantage of our range segmentation algorithm over region growing range segmentation algorithms is the way in which it deals with occlusion or separation of parts. Our method can detect and solve such problems correctly as can be seen from Fig. 6. In this example the planar object is located between two cylinders of the same size whose axis are co-linear. The proposed algorithm correctly detects the existence of such issues.

Surface Library 4

Model 1	$ax^2+by^2+cz^2+dx+ey+fz=1$
Model 2	$ax^2+by^2+cx+dy+eyx=1$
Model 3	$ax^2+bz^2+cx+dz+exz=1$
Model 4	$az^2+by^2+cz+dx+fxz=1$
Model 5	$ax^2+by^2+cx+dy=1$
Model 6	$ax^2+bz^2+cx+dz=1$
Model 7	$ay^2+bz^2+cy+dz=1$
Model 8	$ax+by+cz=1$

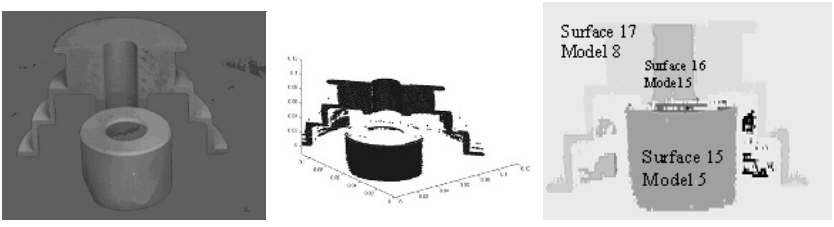

Fig. 3. Intensity image (left), plotted range data (middel) and segmentation result (right). SSC selects model 5 for the perpendicular cylinders to the xy plane (surface 16 and surface 15). The chosen model for the flat surface 17 is model 8. Surface 17, which has two separated planar parts, is an example for occlusion

Fig. 4. Intensity image (left), plotted range data (middle) and segmentation result (right). The perpendicular cylinders to the xy plane are detected correctly (model 5) using SSC. The black region illustrates the missed data. The roofs of three cylinders are in the same hight, and has been correctly segmented by the proposed algorithm

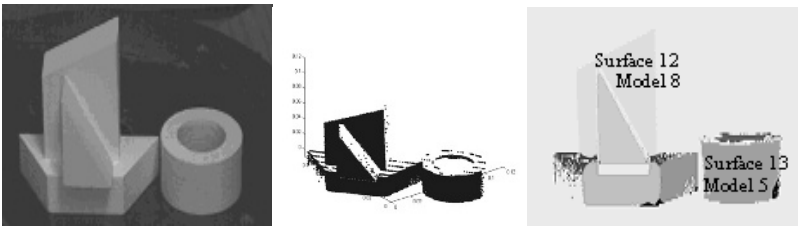

Fig. 5. Intensity image (left), plotted range data (middle) and segmentation result (right). The underlying model for surface 13, which is a cylinder perpendicular to the xy plane is selected to be model 5. For planar surfaces SSC selects model 8 as the underlying model As can be seen from the plotted rang image, despite of having noisy and invalid data, the algorithm is performed

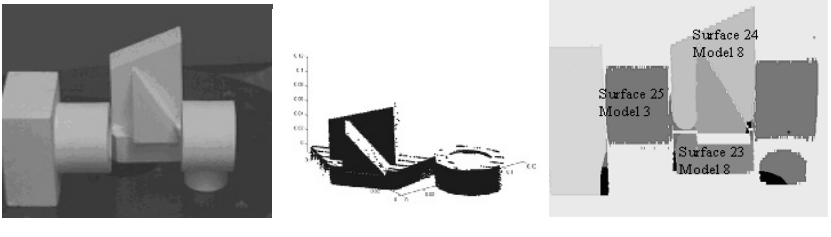

Fig. 6. Intensity image (left), plotted range data (middle) and segmentation result (right). SSC selected model 3 for the cylinders parallel to the xy plane. The underlying surface model for planar surface 24 and 23 and also other planar surfaces in the scene are chosen to be model 8

6 Conclusion

In this paper, we have proposed and evaluated a new surface model selection criterion. Using this criterion, we have also developed a robust model based range segmentation algorithm, which is capable of distinguishing between different types of surfaces while segmenting the objects. The proposed techniques both for model selection and for range segmentation has been extensively tested and have been compared with a wide range of existing techniques. The proposed criterion for model selection and the resulting segmentation algorithm clearly outperforms previously reported techniques**.**

References

1. Arman, F. and Aggarwal, J., Model-Based Object Recognition in Dense Range Images, ACM Computing Surveys, vol. 25, pp. 5–43, Mar, 1993.
2. Bab-Hadiashar, A. and Suter, D., Robust Segmentation of Visual Data Using Ranked Unbiased Scale Estimate, ROBOTICA, International Journal of Information, Education and Research in Robotics and Artificial Intelligence, vol. 17, pp. 649–660, 1999.
3. Besl, P. J. and Jain, R. C., Segmentation Through Variable-Order Surface Fitting., IEEE Transactions on Pattern Analysis and Machine Intelligence, vol. 10, pp. 167–192, Mar, 1988.
4. Boyer, K. L., Mirza, M. J., and Ganguly, G., The Robust Sequential Estimator: A General Approach and its Application to Surface Organization in Range Data, IEEE Transaction on Pattern Analysis and Machine Intelligence, vol. 16, pp. 987–1001, 1994.
5. Bozdogan, H., Model Selection and Akaike's Information Criterion (AIC): The General Theory and Its Analytical Extensions, Psychometrica, vol. 52, pp. 345–370, 1987.
6. Chickering, D. and Heckerman, D., Efficient Approximation for the Marginal Likelihood of Bayesian Networks with Hidden Variables, Machine Learning, vol. 29, no. 2-3, pp. 181–212, 1997.
7. Duncan, J. S., Lee, F. A., Smeulders, A. W. M., and Zaret, B. L., A Bending Energy Model for Measurement of Cardic Shape Deformity, IEEE Transactions on Pattern Analysis and Machine Intelligence, vol. 10, pp. 307–319, 1991.
8. Fan, T. J., Medioni, G., and Nevatia, R., Segmented Descriptions of 3-D Surfaces, IEEE Trans. on Robotics and Automation, vol. 3, pp. 527–538, Dec, 1987.
9. Fitzgibbon, A. W., Eggert, D. W., and Fisher, R. B., High-Level CAD Model Acquisition From Range Images, High-Level CAD Model Acquisition From Range Images, Dept of Artificial Intelligence, Univ. of Edinburgh, 1995.
10. Goldgof, D. B., Huang, T. S., and Lee, H., A Curvature-Based Approach to Terrain Recognition, IEEE Transactions on Pattern Analysis and Machine Intelligence, vol. 11, pp. 1213–1217, 1989.
11. Hoffman, R. L. and Jain, A. K., Segmentation and Classification of Range Images, IEEE PAMI, vol. 9, pp. 608–620, 1987.
12. Hoover, A., http://marathon.csee.usf.edu/range/DataBase.html
13. Hoover, A., Jean-Baptist, G., Jiang , X., J.Flynn, P., Horst, B., Goldgof , D., Bowyer, K., Fggert , D., Fitzgibbon , A., and Fisher, R., An Experimental Comparison of Range Image Segmentation Algorithms, IEEE Transaction on Pattern Analysis and Machine Recognition, vol. 18, pp. 673–689, Jul, 1996.
14. Jiang, X. and Bunke, H., Range Image Segmentation: Adaptive Grouping of Edges into Region, Proceedings of Asian Conference on Computer Vision , Hong Kong, pp. 299–306, 1998.

15. Kanatani, K., What Is the Geometric AIC? Reply to My Reviewers,1987(unpublished).
16. Kanatani, K., Model Selection for Geometric Inference, The 5th Asian Conference on Computer Vision, Melbourne, Australia , pp. xxi–xxxii, January 2002.
17. Kass, M., Witkin, A., and Terzopoulos, D. Snakes: Active Contour Models. In: Anonymous 1987.pp. 269–276.
18. Lee, K.-M., Meer, P., and Park, R.-H., Robust Adaptive Segmentation of Range Images, IEEE Trans. Pattern Anal. Machine Intell., vol. pp. 200–205, 1998.
19. Mallows, C. L., Some Comments on CP, Technometrics, vol. 15, pp. 661–675 , 1973.
20. Marshall, D., Lukacs, G., and Martin, R., Robust Segmentation of Primitives from Range Data in the Presence of Geometric Degeneracy, IEEE Transactions on Pattern Analysis and Machine Intelligence , vol. 23, pp. 304–314, Mar, 2001.
21. Meer, P., Mintz, D., and Rosenfeld, A., Least Median of Squares based robust analysis of Image Structure , Proce. DARPA Image Understanding Workshop, Pittsburgh, PA, pp. 231–254, Sept. 1990.
22. Newman, T. S., Flynn, P. J., and Jain, A. K., Model-based Classification of Quadric Surfaces, CVGIP: Image Understanding, vol. 58, pp. 235–249, 1993.
23. Powell, M. W., Bower, K., Jiang, X., and Bunke, H., Comparing Curved-Surface Range Image Segmentors, Proc. of 6th International Conference on Computer Vision (ICCV), Bombay,India, pp. 286–291, 1998.
24. Rissanen, J., Universal Coding, Information, Prediction and Estimation, IEEE Trans. Inf. Theory, vol. 30, pp. 629–636, 1984.
25. Rissanen, J., Modeling by Shortest Data Description, Automatica, vol. 14, pp. 465–471, 1978.
26. Rousseeuw, P. J., Least median of squares, Journal of the American Satistical Association, vol. 85, pp. 115–119, 1984.
27. Timoshenko, p. S. and Krieger, S. W. Theory of Plates and Shells. In: Chapter 2, Pure Bending of Plates, eds. Timoshenko, p. S. and Krieger, S. W. McGraw-Hill, 1959.pp. 46–47.
28. Trucco, E. and Fisher, R. B., Experiments in Curvature-based Segmentation of Range Data, IEEE Transactions on Pattern Analysis and Machine Intelligence, vol. 17, pp. 3177–182, 1995.
29. Van Vliet, J. L. and Verbeek, W. P., Curvature and Bending Energy in Digitized 2D and 3D Images, Proceedings of 8th Scandinavian Conference on Image Analysis, Toromso,Norway , pp. 1403–1410, 1993.
30. Young, I. T., Walker, J. E., and Bowie, J. E., An analysis technique for biological shape. I. Information Control, vol. 25, pp. 357–370, 1974.